AEJ
Alexandria Engineering Journal

Estimation of local scour depths around abutments using artificial neural network model

H.M. Moghazy, H.M. Nagy and G.Y. Lazem
Irrigation and Hydraulics Eng. Dept., Faculty of Eng., Alexandria University, Alexandria, Egypt

Local scour occurs when the local flow near the structure is strong enough to remove bed material around it. Most of previous methods to predict the local scour depth are based on the regime approach, dimensional analysis, analytical, experimental or semi empirical approach. All of these methods depend on much simplification of analysis in order to overcome the large number of parameters. The main objective of the present study is to develop a new approach for predicting the local scour depths around abutments. Artificial Neural Networks, (ANN), model was used to investigate the problem. The concept of artificial neural networks is an advanced topic that provides a strong tool for estimating the missing information to be used. In this study, the parameters that affect local scour depth were investigated, based on the previous data by others, in order to determine the dominant parameters to be used in the ANN model. By using the error analysis, the mean and standard deviation were determined to calibrate the model. A sensitivity analysis was used to investigate the effect of the different parameters affecting local scour depth on the ANN model. The most effective parameters were determined. A comparison was made among the obtained results from the ANN model, the regression analysis and the previous formulas to determine the accuracy of the model results. The study shows that ANN model gives good prediction of the local scour depth around abutment. The results are close to the corresponding previously measured values compared with other formulae.

يحدث النحر الموضعي عندما يكون التدفق قرب المنشأ قويا لازاله مكونات القاع مما يشكل خطوره علي أساسات المنشأ. وتستند اغلب الطرق المختلفة لحساب عمق النحر الموضعي علي المدخل التحليلي أو النصف تجريبي. و نظرا لوجود العديد من العوامل المؤثرة في دراسة النحر فان معظم هذه الطرق تعتمد علي تبسيط هذه المشكلة بحذف بعض العوامل مما يؤثر علي دقه حساب عمق النحر. الغرض من البحث تطبيق نموذج شبكه الأعصاب الاصطناعية في استنتاج قيم أعماق النحر الموضعي حول الأكتاف ودراسة العوامل المؤثرة في عمليه النحر. وفي هذه الدراسة تم تحديد العوامل المختلفة المؤثرة علي النحر طبقا للدراسات السابقة وتجميع البيانات من الأبحاث الموثقة والمنشورة لاستعمالها في هذا النموذج. بعد تعريف البرنامج بالمدخلات تم اختبار قدرته علي استنتاج قيمه عمق النحر الموضعي. ووجد عند تشغيل النموذج انه يعطي قيم متقاربة مع القيم المقاسه في التجارب المعملية. ولمعايره نتائج النموذج تم استعمال نظريه تحليل الخطأ (Error Analysis) عن طريق تحديد القيمة المتوسطة والانحراف المعياري للخطأ. وتم مقارنه هذه النتائج بنتائج معادلات سابقه لنفس البيانات ووجد أن النموذج يعطي نتائج قريبه من النتائج المعملية مقارنه بالمعادلات. وبتطبيق هذا البرنامج تم تحديد أهم المتغيرات المؤثرة في ظاهره النحر الموضعي والتي تؤثر علي كفاءة البرنامج في تحديد قيم عمق النحر الموضعي. تم أيضا مقارنه هذه الطريقة بطريقه التحليل الترددي (Regression Analysis) ووجد أن برنامج (Artificial Neural Network) يعطي نتائج أفضل.

Keywords: Local scour depth, Abutment, Artificial neural network, Regression analysis, Shear stress

1. Introduction

Local scour is the scour around an obstruction. It is a result of the flow pattern created by the presence of the obstruction. It is confined to small area around the obstruction and associated with three dimensional flow and vortex system. Local scour may be subdivided into two categories. They are clear water scour and live bed scour. When local scour around abutments occurs in the absence of sediment transport it is commonly known as clear water scour. The moving of bed material from the scour hole is practically undisturbed by the flow and no sediment is supplied to the scour hole to replenish the amount which has been removed. Sediment is removed only near the abutment where the shear stresses on the boundary are greater than critical shear stress τ_c. The bed material

upstream of the scour area is at rest and thus no sediment is supplied to the scour hole to replace the amount, which has been eroded. Clear water scour may be regarded as being the threshold condition of live-bed scour. For this case, the maximum clear water scour depth is generally 10% more than that due to live-bed scour as shown in fig. 1. For design purpose, clear water scour should be considered the worst condition more than live bed scour. Local scours at bridge abutments, piers and spur-dikes have been a subject of interest and importance to many researchers. Gill [1] studied the local scour around spur dikes experimentally. He concluded that depth of equilibrium scour is affected by the size of bed material. Rate of scour development of the fine sand was higher than that of coarse sand. Depth of equilibrium scour is also affected by the depth of uniform flow upstream of the scour location and the depth of maximum scour occurs when the sand bed upstream of the spur dike is at the threshold of movement. Melville [2] presented laboratory data from various researchers' experiments to demonstrate their effects on scour depth. He included sufficient data of abutment length, flow depth, abutment shape and alignment, scour data for the effects of sediment characteristics, flow intensity and approach channel geometry.

He obtained the following relationship between scour depth and some of the parameters that affect it.

$$d_s = 2k_s L \quad L/Y_o < 1, \tag{1}$$

$$d_s = 2K_s^* K_\theta^* (Y_o L)^{0.5} 1 \le L/Y_o \le 25, \tag{2}$$

$$d_s = 10\, k_\theta\, Y_o \quad L/Y_o > 25. \tag{3}$$

Dey and Barbyuiya [3] presented an investigation for the scour around vertical wall, wing wall and semicircular abutment. Experiments were for clear water scour and uniform sediments to compute the time variation of scour depth in an evolving scour hole. They concluded equations by regression analysis:

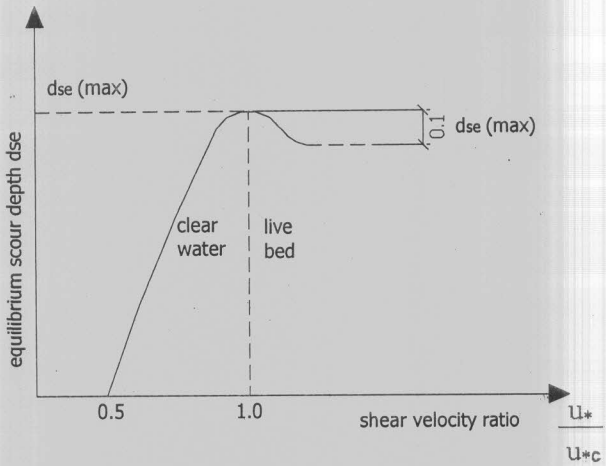

Fig. 1. Variation of equilibrium scour depth with shear velocity ratio (after Tey, 1984).

$$\frac{d_s}{L} = 8.319\ F_e^{0.312} \left(\frac{y_0}{L}\right)^{0.101} \left(\frac{y_o}{L}\right)\left(\frac{L}{d_{50}}\right)^{-0.231} . \tag{4}$$

Where F_e is excess abutment Froude number, $=U_e/(\Delta g l)^{0.5}$, $U_e=(U_0-\xi U_{oc})$ is the approaching velocity and ξ is constant = 0.55 for wing wall abutment. Tey [4] investigated the effect of flow depth on the maximum depth of local scour at bridge abutments. Kandasamy [5] investigated the effect of flow depth and abutment length on local scour depth at threshold condition $U*/U*_c$ = 1.0, and the effect of shear velocity ratio on local scour depth. Kwan [6] investigated the effect of flow depth changes on the velocity field and mapped the three dimensional flow patterns in the abutment vicinity under clear water scour condition and presents the following equation.

$$\frac{d_{sm}}{y_o} = 0.32 + K\left[\frac{L}{y_o}\right]^{0.5} . \tag{5}$$

Lim [7] carried out experimental investigations to present a semi empirical analysis to determine the maximum local scour depth for clear water scour and to check the developed relationship against laboratory data from his study and many other data. He concluded the following equation.

$$\frac{d_s}{y_o} = K_s(0.9 \times -2). \quad (6)$$

Rahman and Muramoto [8] developed a simplified analytical model for the prediction of the maximum scour depth around spur-dike like structure based on continuity relation between the inflow and the outflow in the restricted flow concentration region of a scour hole.

Froehlich [9] modifies equation for estimating the scour depth

$$\frac{d_s}{y_o} = 0.78K_s\, k_\theta \left(\frac{L}{y_o}\right)^{0.63} F_N^{1.16} \left(\frac{y_o}{d_{50}}\right)^{0.43} \sigma_g^{1-.87}. \quad (7)$$

Nagy [10] in his study for the scour depth near emerged vertical wall spur dike, concluded equation by the regression analysis method

$$\frac{d_s}{y_o} = 3\frac{(L/y_o)^{0.42}(\sin\alpha)^{0.717}}{(d_{50}/y_o)^{0.277}} F_N^2. \quad (8)$$

2. Review on artificial neural network model

An artificial neural network is an information-processing system. A neural net consists of a large number of simple processing elements called neurons. Each neuron is connected to other neurons by means of directed communication links each with an associated weight. The weights represent information being used by the net to solve the problem. Each neuron has an internal state called its activation function or activity level, which is a function of the inputs. A neuron sends its activation function as a signal to several other neurons. The neuron can send only one signal at a time and that signal is broadcasted to other several neurons

A biological neuron has three types of components. They are dendrites, soma (cell body), and axon as shown in fig. 2. The signal from one neuron is passed into another by means of a connection between the axon of the first and a dendrite of the second. This connection is called synapse. Axons often synapse onto the trunk of a dendrite, but they can also synapse directly onto the cell body. The signals are electric impulses that are transmitted across a synaptic gap by means of chemical process. The action of the chemical transmitter modifies the incoming signal (typically, by scaling the frequency of the signals that are received) in a manner similar to the action of weights in an artificial neural network. The soma, or cell body, sums the incoming signals, when sufficient input is received, the cell fires; by means of transmitting a signal over its axon to other cells. It is often supposed that a cell either fires or doesn't at any instant of time, so that transmitted signals can be treated as binary.

A neural network is characterized by its pattern of connections between the neurons. Fig. 3 shows an example of a simple neuron.

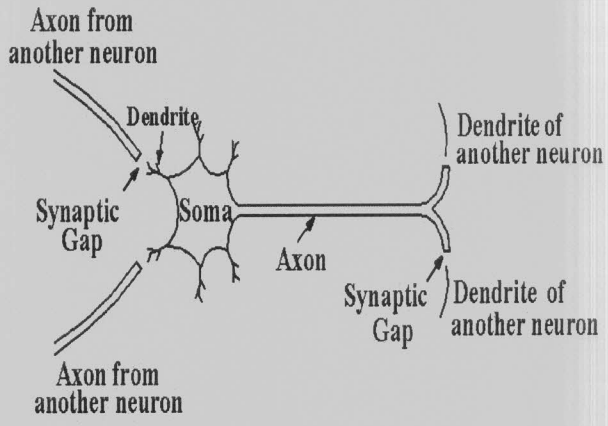

Fig. 2. Biological neuron.

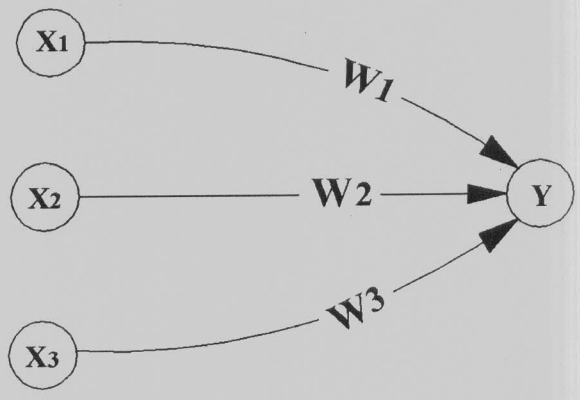

Fig. 3. A simple artificial neuron.

2.1. Advantages of using artificial neural network models

Neural networks are useful when the underlying problem is either poorly defined or not clearly understood. Their application does not require knowledge of the underlying process beforehand. They are advantageous when specific solutions do not exist to the problem posed. A small amount of errors in the input does not produce significant change in the output because of distributed process. The artificial neural networks are very fast even on regular PCs. A very important feature of these networks is their adaptive nature where "learning by example" replaces "programming or making functions" in solving problems.

Use of ANN techniques to solve civil engineering problems began in the late 1980s. Rumelhart et al. [11] played a major role in the reemergence of neural networks as a tool for solving problems. Flood and Kartman, [12] used ANN to simulate and forecasting problems in water resources. They include works of French et al. [13] to forecast rainfall inspect and time domain. Nagy et al. [14] used an artificial neural network model to estimate the natural sediment discharge in rivers in terms of sediment concentration.

3. Parametric analysis

The analysis of abutment local scour depth involves a large number of interacting parameters that influence the scour process. The data used in the study is collected to cover a wide range of data as shown in table 2. The relationship between the depth of local scour and the parameters which affect on it can be summarized as follows:

- $d_s = f$ (flow, fluid, bed material, abutment and time) in which;
- The flow of fluid is characterized by its mean depth y_o, energy slope s_o, the gravitational constant g, and the channel width B.
- The fluid can be characterized by its density ρ, and kinematical viscosity ν. Both ρ and ν are functions of temperature.
- The bed material is characterized by its specific gravity S_s and the mean diameter d_{50}. The degree of uniformity of the particle size distribution can be defined by its standard deviation σ_g.
- The abutment is largely determined by its shape factor K_s, the length of abutment perpendicular to flow (projected length) L and the angle of approach flow to the abutment θ.
- Local scour is time dependent. Scour depth increases with time to reach an equilibrium state.

For steady uniform flows, constant temperature and a cohesionless granular spherical bed material, the local scour depth can be formulated as

$$d_s = f(L, B, y_o, U^*, g, \rho, \nu, S_s, d_{50}, \sigma_g, K_s, \theta, t). \quad (9)$$

3.1. Effect of flow depth

The influence of flow depth is assumed to depend on the ratios of U_*/U_{*c} and y_o/L. Most researchers state that for a constant value of U_*/U_{*c} the equilibrium scour depth increases with increasing flow depth but in a decreasing rate and becomes independent at higher values of flow depth. [Melville [15]]. Tey [4] and Dongol [16] found from their experiments that the scour depth d_s/y_o increases with increasing flow depth y_o/L. They found also that the scour depths for vertical wall abutment are higher than that of wing-wall.

3.2. Effect of Froude number

The Froude number is a significant parameter which adequately accounts for the effect of flow characteristics on the maximum scour depth. The relationship between the Froude number and scour depth. According to Tey [4], Kwan [6], Kandasamy [5], Rahman et el. [17] and Dey and Barbyuiya [3] indicate that The scour depth increases as the value of Froude number increases

3.3. Effect of sediment size

The sediment characteristics are presented by the median diameter d_{50} for uniform sediment.

Gill's [1] results for two sand sizes (d_{50}1.52 and 0.914 mm) indicate that for the same value of $U_*/U_{*c} < 1$, the scour depth is

deeper for the coarser sand than for the fine sand. From Tey [4], Kwan [18] and Rahman and Muramoto [8] experiments it can be concluded that for L/d_{50} >100 the scour depth increases with an increase of sediment size.

3.4. Effect of sediment gradation

The variation of particle size distribution was generally found to have a pronounced effect on local scour depth. Non-uniform sediment mixtures (σ_g > 1.5-2) have been reported to produce lower scour depth than uniform sediment. The non-uniform sediments are known to reduce the resistance to flow. The coarser fraction deposits as a protective layer at the bottom of the hole prevent further removal of the bed material.

From previous studies under clear water scour conditions, Ahmad [19] and Wong [20] found that for a constant shear velocity ratio U_*/U_{*c} the rate of scour and the maximum equilibrium scour depth decreases as the standard deviation of the sediment mixture increases. This trend is a consequence of the armor layer formation of a more resistant coarser particle layer from the coarser fraction of the non-uniform mixture.

3.5. Effect of abutment length

Investigations of the influence of abutment length perpendicular to flow L have been correlated in terms of either L/B or L/y_o. There is a general agreement among investigators that local scour depth increases with the increase of L. When the length L increases the backwater also increases. For a constant flow rate, the higher the backwater, the larger the reduction in bed shear stress upstream of the abutment.

Based on his experimental work, Kwan [18] draws the streamlines pattern of five different abutment lengths. He observed that the streamlines separate on approaching the nose of the abutment. As the length L is increasing, a greater proportion of the streamlines is contracted at the nose, consequently resulting in greater scour.

According to Tey [4], Kwan [6], Kandasamy [5], Rahman et al. [16] and Lim [7], for a constant value of Froude number, the scour depth increases gradually with increasing the ratio L/B for vertical wall and wing wall abutment.

3.6. Effect of abutment shape

Most investigators indicated that there is influence of abutment shape on the scour depth. They show that the blunter the obstruction, the deeper will be the scour depth. This is because of the difference in the flow pattern generated for each kind of abutment. Melville [2] presented shape factors for different abutment shapes

3.7. Effect of abutment alignment

Researchers found that the scour depth increases with increasing the angle of alignment θ fig. 4. As expected, the angle θ=30° produces the least scour depth. Kwan [19] analyzed several angles of alignment and found that the abutment alignment is defined by the angle θ. From the experiments, it was found that the scour depth increases with increasing of θ. Using the perpendicularly aligned abutment angle θ= 90° as a reference, abutments pointed upstream are found to produce larger scour depths

Melville [2, 15] divided the alignment factor for short abutments, long abutments and intermediate ones. He shows that the effect of alignment on scour depth disappears for short abutment $L/y_o \leq 1$. He obtained alignment factors K_θ for different angles of alignment.

4. Selecting the parameters of ANN

Local scour is time dependent process. At equilibrium, the parameters will be normalizing and will be considered all the factors that affect local scour depth.

4.1. The flow characteristics

This can be expressed by flow velocity $\frac{U_o}{u^*}$,

Shear stress $\psi = \frac{y_o \quad S_o}{(S_s - 1)d_{50}}$, Froude number,

where $F_N = \frac{U_o}{\sqrt{g\, y_o}}$.

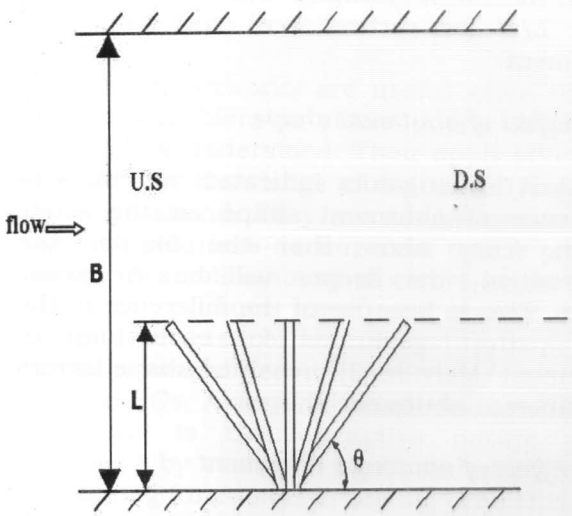

Fig. 4. Definition sketch of abutment skewness.

4.2. The abutment shape and alignment

Melville [2] selected the vertical wall abutment as the primary shape and therefore K_s = 1. He plotted data for the effects of abutment alignment with respect to flow and made a table for the data. He concluded that as the abutment length perpendicular to flow L increases, the scour depth increases.

4.3. The sediment size and gradation

For clear water scour, Tey [4] mentioned that Ettema [21] defined the influence of sediment size on scour depth at circular piers for uniform sediments that scour depth increases with the relative sediment size L/d_{50} up to L/d_{50}= 50. For L/d_{50} > 50, d_s is independent of the sediment size. Dongol [16] found that the influence of relative sediment size on scour depth is the same for both piers and abutments. All the previous experiments were applied for uniform sediments that can be described by the geometric standard deviation σ_g.

Based on the previous studies, the final developed expression for local scour depth is:

$$d_s / Y_o = f(\psi, \frac{U_o}{U^*}, F_N, k_s, K_\theta, L/B, \sigma_g, L/d_{50}) . \quad (10)$$

4.4. Multilayer network

A multilayer net is a net with one or more layers of nodes (the so-called hidden units) between the input units and the output units. Typically, there is a layer of weights between two adjacent levels of units (input, hidden, or output), as shown in fig. 5 Multilayer nets can solve more complicated problems than can single-layer nets, but training may be more difficult.

4.5. Back propagation neural net

Rumelhart et el. [11] played a major role in the reemergence of neural networks as a tool for solving problems. The back propagation or the generalized delta rule is simply a gradient descent method to minimize the total square error of the output computed by the net.

The aim is to train the net to achieve a balance between the ability to respond correctly to the input patterns that are used for training and the ability to give reasonable response to input that is similar, but not identical, to that used in training.

4.6. Training the network and verification of results for vertical wall abutment

Table 1 presents the range of data used in training and verification for vertical wall abutment. The network was set up with eight parameters and the local scour depth is considered the output for 142 patterns. Therefore, the input layer contains eight neurons, while the output layer contains one. Between the two layers, there is another hidden layer contains a suitable number of neurons. The network was trained with 71 patterns. The number of neurons in the hidden layer and the parameters α ε were determined by calibration through several computer run tests. The best fitting of the measured and estimated data was found to be for number of neurons in the hidden layer equals 8, the parameter α equals 6 and the parameter ε equals 0.01. After the network is calibrated the other half of 71 patterns was added without inserting the output layer d_s/y_o and to be predicted by the program.

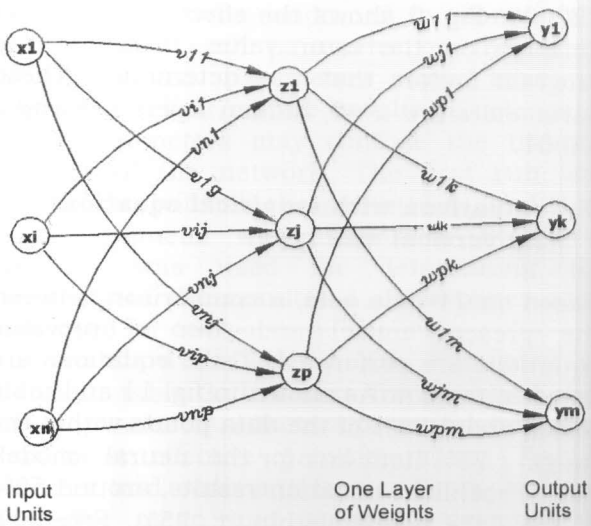

Fig. 5. A multilayer neural net.

4.7. Calibration of model parameters

The number of neurons on the hidden layer, the value of learning rate parameter and the value of shape factor of sigmoid function must be assumed first before the training. To determine the exact model parameters which agree with the measured one, these parameters were calibrated.

4.8. Error analysis

The estimated values were compared with the measured ones. A discrepancy ratio, $D_r = d_{se} / d_{sm}$ was used for comparison, where d_{se} is the estimated local scour depth and d_{sm} is the measured one. The mean value and the standard deviation σ are expressed as:

$$D_r = \sum_{i=1}^{n} D_{ri} / N , \qquad (11)$$

and

$$\sigma = \sqrt{\sum_{i=1}^{N} (D_{ri} - Dr) / N - 1} . \qquad (12)$$

where N is the number of tested data

4.9. Calibration of steepness α

The factor α affects the behavior of the sigmoid function as shown in fig. 6. The changing of the parameter α in the sigmoid function affects the training results. The best results of training are obtained at a value = 6. Where the mean =1.000199, σ =0.038. Fig. 7 shows the change in accuracy of results by changing α.

Table 1
Range of data used in learning and verification for vertical wall abutment

Variables	range	Variables	range
Shear stress ψ	0.025-0.348	Alignment factor K_θ	0.94-1.07
Flow velocity ratio $\frac{U_o}{U_*}$	0.015-21.377	Contraction ratio L/B	0.044-0.593
Froude number F_N	0.149-0.810	Sediment standard deviation σg	1.17-1.38
Shape factor K_s	0.75-1.0	Sediment size L/d_{50}	12.903-647.059

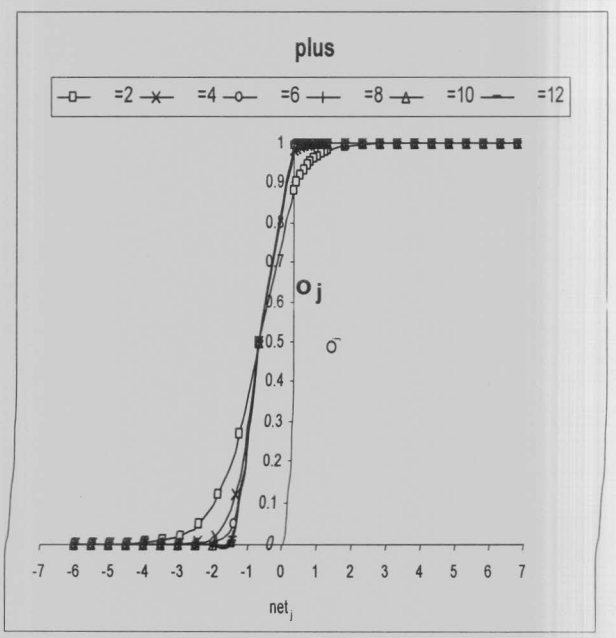

Fig. 6. Effect of α on the activation function.

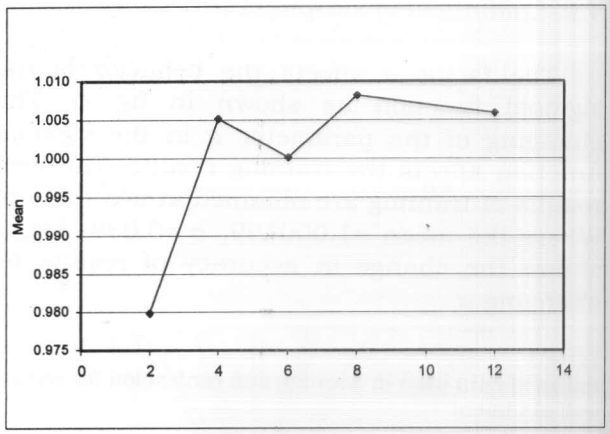

Fig. 7. Effect of α on the model results

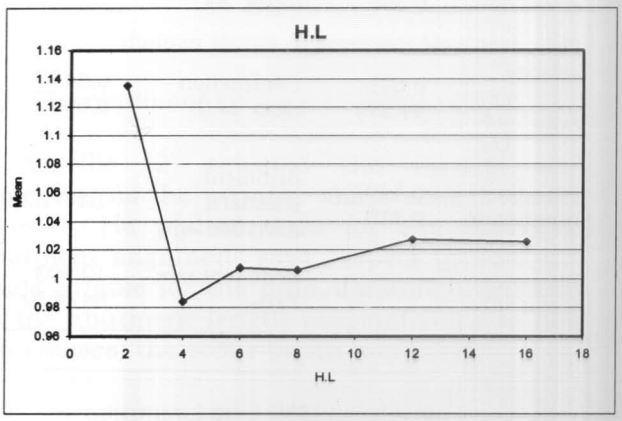

Fig. 8. Effect of hidden layers on the model results.

4.10. Effect of hidden layers

The number of neurons in the hidden layers affects the performance of the model. The best results of training are obtained for number of hidden layers = 8 as shown in fig. 8.

4.11. Effect of epsilon ε

The learning rate ε affects on the model results. The value of epsilon that gives the best results is = 0.01.

4.12. Effect of number of iterations

Good performance of ANN is obtained when the iteration number increases up to 130000. Fig. 9 shows the effect of number of iteration on the error value, based on the program factors that was determined. These parameters are α =6, hidden layers = 8 and ε = 0.01.

5. Comparison with empirical equations for vertical wall type

Based on 71 data sets, a comparison between the present model and four of previous equations are performed. These equations are listed in table 4. As shown in fig. 11 and table 5 that about 95% of the data points within the range ± 25% limit line for the neural model. For Froehlich equation results, around 56% of the data points within ± 25%. Froehlich equation gives a high value of standard deviation. Lim equation results give about 72% of the data points within ± 25%, and about 80% within the range ± 50%. Lim depends basically in his equation on the parameters L and y_o. Melville equation gives about 50% in the ± 25% limit line. Melville depends on many simplifications in his equation, the effect of Froude number, particle size and particle standard deviation and the bed shear stress was not considered. Nagy equation gives about 47% with the range ± 25% limit line. By comparing the results from ANN model with other equations, the mean of the ANN is the least one and equal to1.04.

5.1. Sensitivity analyses

The estimated values were compared with the measured ones. The best results of training the model are for mean of 1.000199 and standard deviation of 0.38. A comparison between measured and estimated local scour depth are presented in fig. 10. The figure shows that the agreement between the measured and calculated scour depths is almost identical.

5.2. Effect of different parameters on the accuracy of the ANN model

The variables shown in table 3, which used in the analysis of ANN program, were assumed to be the most effective parameters.

Several trials were conducted to examine the sensitivity of each parameter on the model results. Some parameters may have no significant effect on the results. Existence of other parameters may confuse the training process of the network. The first run was carried out with all the parameters, and then each parameter was eliminated. Statistical analysis was used for determining the accuracy of the results. A discrepancy ratio was used for comparison. The mean value and the standard deviation σ are calculated as listed in table 3. It seems from table 3 that every parameter affects the model accuracy but most effective parameters are Froude number and sediment factor. Table 3 shows also the mean and standard deviation of eliminating each parameter and the accuracy of the model. From table 3, it appears that the model is more sensitive to the parameters ψ , F_N and L/d_{50}. When eliminating L/d_{50}, the mean was doubled and the standard deviation increases to a very high value. This indicates that the sediment size is an important parameter in the scour prediction. When eliminating ψ and F_N the mean change with about 8% but the standard deviation changed substantially. The parameters $\frac{U_o}{U*}$, σ_g, K_s, K_θ and L/B have less effect on the results when eliminating. The less parameter that the model had a negligible affect is the sediment standard deviation. In case of removing this parameter, the standard deviation of the program increases by about 16%.

5.3. *Training the network and verification of results for local scour around wing wall abutment*

From the collected data sets, the dimensionless data are processed into the following form to cover the selected parameters. Table 6 presents the range of data used in learning and verification for wing wall abutment case. The network was set up with six parameters and the local scour depth as the output. Therefore, the input layer contains six neurons, while the output layer contains one. Between the two layers, there is another hidden layer contains a suitable number of neurons. The network was trained with 158 patterns. The numbers of neurons in the hidden layer, the parameters α, ε were determined by calibration through several computer run tests. The best fitting of the measured and estimated data is for number of neurons in the hidden layer equals 2, the parameter α is equal to 14 and the parameter ε is equal to 0.01. After the network is calibrated well, the other half of 158 patterns was added without the output layer d_s/Y_0 to be predicted by the program.

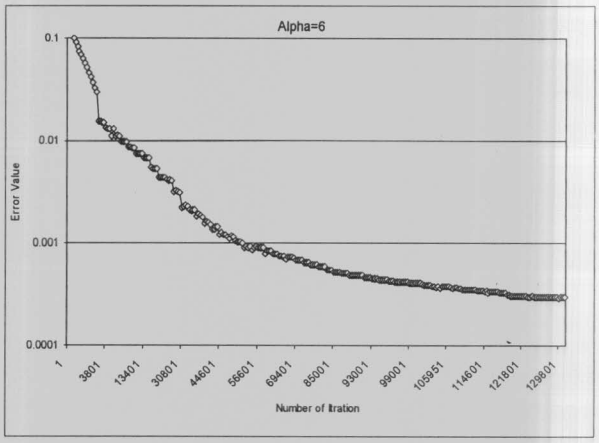

Fig. 9. Effect of iteration number on the model results.

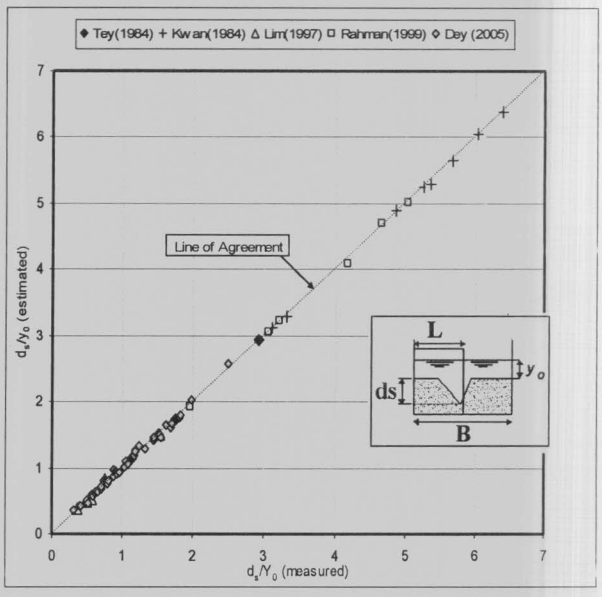

Fig. 10. Comparison between measured and estimated scour depth for vertical wall abutment.

Table 2
Summary of the experimental data

Researcher	Abutment type	σg	d_{50} (mm)	F_n	L (mm)	Y_o (mm)	θ degree	No. of points
Tey (1984)	S.C.E [1]	1.26	0.82	0.19-0.38	165-302	50-350	90	5
Kwan (1984)	S.C.E	1.28-1.30	0.85	0.31-0.41	314-1400	50,100	45-135	17
Lim (1997)	V.W [2]	1.25	0.94	0.15-0.27	50-150	150	90	11
Rahman (1999)	V.W	1.28	0.14	0.54-0.81	100-200	14.3-21.5	90	9
Dey and Barbyuiya (2005)	V.W	1.17-1.38	0.26-3.10	0.18-0.48	40-120	62-250	90	99
Tey (1984)	W.W [3]	1.26	0.82	0.17-0.38	296-600	50-500	90	24
Kandasamy (1989)	W.W	1.30	0.90	0.23-0.56	380-1180	20-280	90	30
Kwan (1988)	W.W	1.30	0.85	0.26-0.42	475	50-200	90	5
Dey and Barbyuiya (2005)	W.W	1.17-1.38	0.26-3.10	0.17-0.48	40-120	59-250	90	99
Tey (1984)	T.S	1.26	0.82	0.19-0.38	302	50-350	90	7
Tey (1984)	S.T [5]	1.26	0.82	0.19-0.38	295-445	50-350	90	6

[1] Semicircular end
[2] Vertical wall abutment
[3] Wing wall abutment
[4] Triangle shape abutment
[5] Spill- through abutment

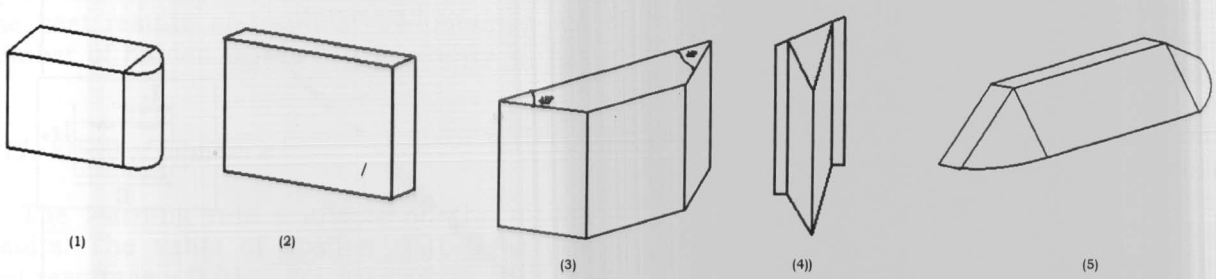

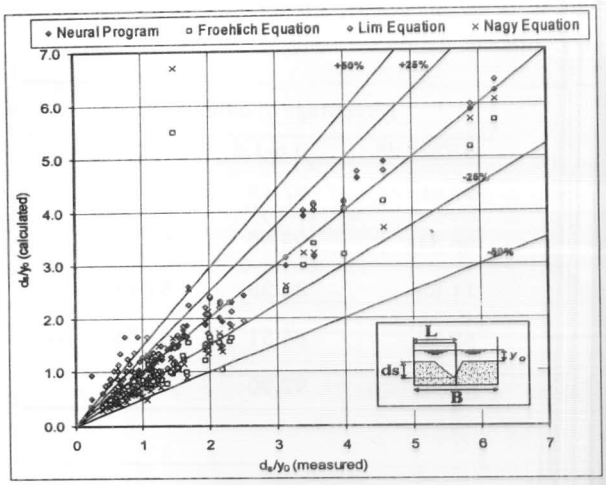

Fig. 11. Comparison between ANN model and some equations.

Table 3
Effect of parameters on results accuracy (number of data sets =142)

Input of the parameters	Mean	Standard deviation
the full parameters	1.02	0.12
Eliminating "ψ"	1.05	0.95
Eliminating "$\frac{U_o}{U_*}$"	0.93	0.50
Eliminating "F_N"	0.96	1.12
Eliminating "K_s"	0.87	0.42
Eliminating "$K\theta$"	1.02	0.62
Eliminating "L/B"	0.98	0.57
Eliminating "σg"	0.93	0.32
Eliminating "$L/d50$"	1.99	3.27

5.4. Effect of epsilon ε

The best results for the model are obtained for epsilon value = 0.01.

5.5. Effects of hidden layers

The number of hidden layers affects the performance of the model. The best results of training are obtained for number of hidden layers=2. Fig. 13 shows that the mean value changes by changing the number of neuron in the hidden layers.

Table 4
Summary of equations used in comparison

Lim [7]	$\frac{d_s}{y_o} = K_s(0.9 \times -2)$
Melville [2]	$L/\ y_o \le 1 \quad d_s = 2\ L$ $1< L/y_o < 25\ d_s = 2\ (\ Ly_o)^{0.5}$ $1< y_o \ge 25\ \ d_s = 10\ \ y_o$
Froehlich [9]	$\frac{d_s}{y_o} = 0.78\ K_s\ k_\theta \left(\frac{L}{y_o}\right)^{0.63} F_N^{1.16} \left(\frac{y_o}{d_{50}}\right)^{0.43} \sigma g^{-1.87}$
Froehlich [9]	$\frac{d_s}{y_o} = 3\frac{(L/y_o)^{0.42}(\sin\alpha)^{0.717}}{(d_{50}/y_o)^{0.277}} F_N^2$

5.6. Calibration of steepness α

The factor α affects the behavior of the sigmoid function. The changing of the parameter α in the sigmoid function affects the training results. The best results of training are obtained for the value 14, where the mean =1.0034, σ = 0.20. Figure 12 shows the changes in the accuracy of results by changing α.

5.7. Effect of number of iteration

The error value decreases as the number of iteration increases as shown in figure 14. The good performance of ANN is obtained when the iteration number increases until a value of approximately 129951.

5.8. Sensitivity analysis

The estimated values were compared with the measured ones. The best results of training the model were obtained for mean of 1.0034 and standard deviation of 0.20 as shown in figure 15. The data sets are almost compatible with the agreement line. The results for the estimated values are of mean =1.004 and standard deviation =0.22.

Table 5
Accuracy of formulas for local scour depths of vertical wall type (number of data sets=71)

Method	Mean (eq.11)	Standard deviation (eq.12)	Percentage of data in range		
			0.75-1.25	0.5-1.5	0.25-1.75
Present ANN	1.04	0.16	95.66	97.18	98.59
Froehlich eq. [9]	0.91	0.54	56.34	92.96	94.37
Lim eq. [7]	1.21	0.45	71.83	80.28	91.55
Melville eq.[2]	1.21	0.48	50.70	84.51	91.55
Nagy eq.[10]	0.98	0.80	46.48	92.96	94.36

Table 6
Range of data used in learning and verification of wing wall type

Variables	Range	Variables	Range
Shear stress ψ	0.027-1.41	Alignment factor K_θ	0.75
Flow velocity ratio $\frac{U_o}{U^*}$	12.041-21.377	Contraction ratio L/B	0.044-0.575
Froude number F_N	0.169-0.559	Sediment standard deviation σ_g	1.17-1.38
Shape factor K_s	1.0	Sediment size L/d_{50}	12.903- 1533.33

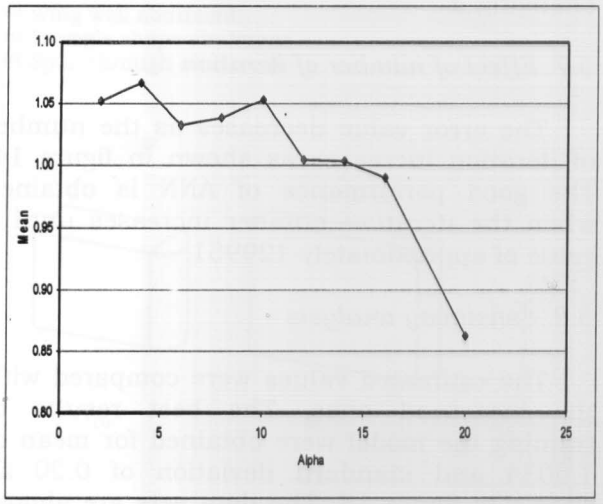

Fig. 12. Effect of α on the model results.

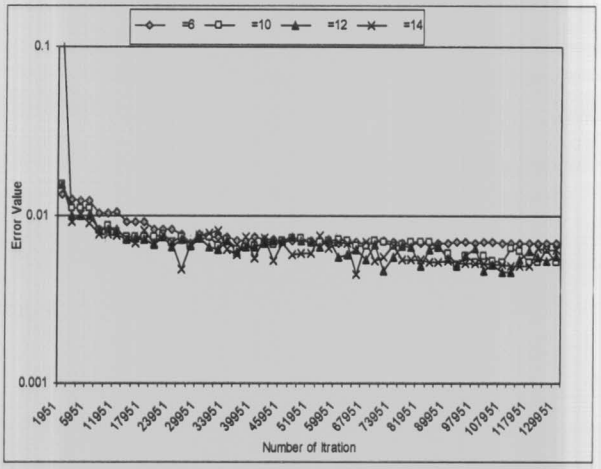

Fig. 13. Effect of hidden layers on the model results.

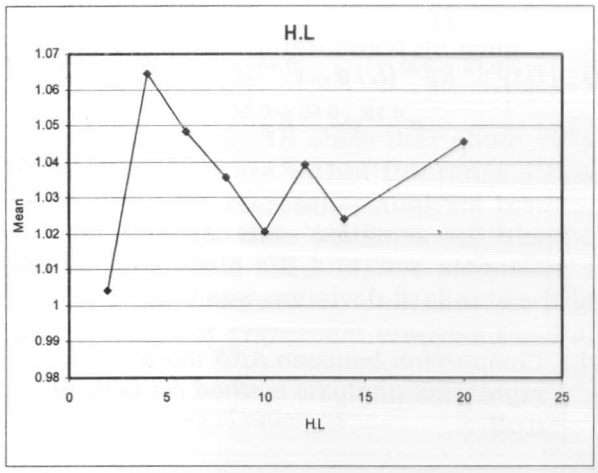

Fig. 14. Effect of iteration number on the model results.

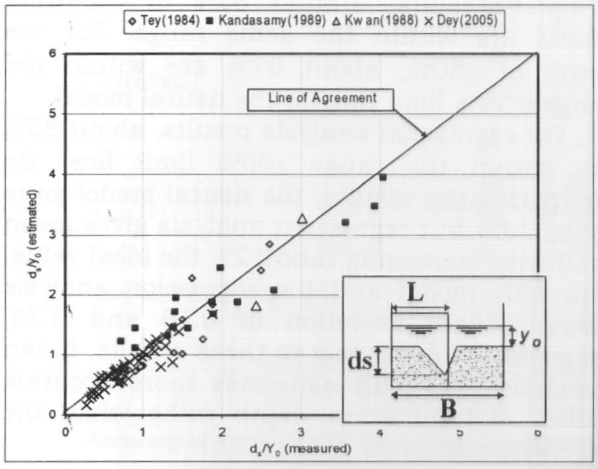

Fig. 15. Comparison between measured and estimated scour depth for wing wall type.

5.9. Effect of different parameters on the accuracy of ANN model

Several experiments were conducted to examine the sensitivity of each parameter on The first run was carried with all the parameters then each parameter was eliminated from the group. Statistical analysis was used for determining the accuracy of the results. The mean value and the standard deviation σ are calculated. It seems from table 7 that the mean affected by eliminating all the parameters and the standard deviation. This indicate that the parameters are important in the model.

Table 7
Effect of parameters on results accuracy (number of data sets=158)

Input of the parameters	Mean	Standard deviation
the full parameters	1.0039	0.21
Eliminating "ψ"	1.09	0.31
Eliminating "$\frac{U_o}{U_*}$"	1.08	0.28
Eliminating "F_N"	1.08	0.26
Eliminating "L/B"	1.005	0.26
Eliminating "σ_g"	1.02	0.22
Eliminating "$L/d50$"	1.08	0.27

5.10. Comparison with empirical equations for wing wall type

A comparison between the present model and five of previous equations as shown in table 8 on the same 78 data was performed to determine the accuracy of the formulas. Fig. 16 and table 9 show that about 72% of the data points within the range ± 25% limit line and about 97% of the data points within the range ± 50% limit line for the neural model. For Froehlich equation results, around 46% of the data points are within± 25% and about 98% of the data points within the range ± 50% but the data is under predicting. Froehlich equation gives a low value of the mean. Lim equation results gives about 56% of the data points within±25% and about the model results. 90% within the range ± 50%. Lim depends basically in his equation on the parameters L and y_o. Melville equation results give about 38% in the ± 25% limit line and about 66% within the range ± 50%. Melville depends on many simplifications in his equation, the effect of Froude number, particle size and particle standard deviation and the bed shear stress were not considered. Dey equation results gives about 80% with the range ± 25% limit line and about 86% within the range ± 50%. Dey used the regression analysis to obtain his equation. His results are

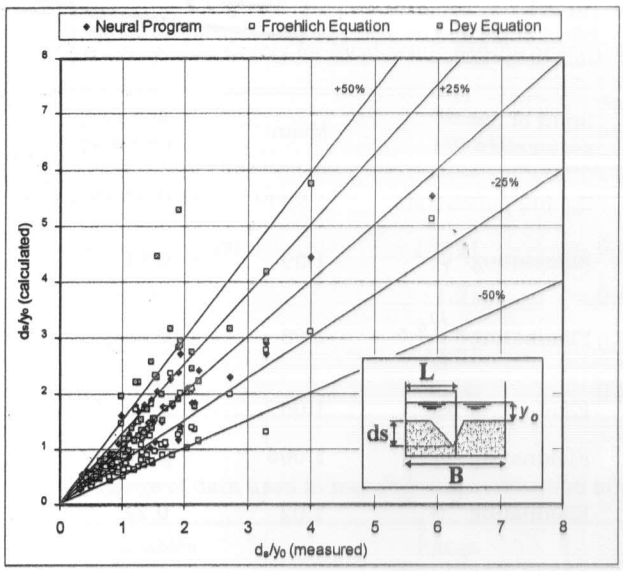

Fig. 16. Comparison between ANN and some equations.

good in the range ± 25% and increases slightly at ± 50% range. The mean and standard deviation in the neural model are better than Dey equation. Kwan equation gives about 40% within the range ± 25% and about 67% within the range ± 50%. Kwan predicted the equation in a narrow range of data. By comparing the results from ANN model with other equations according to the results, the mean of the ANN is the least one and equal to1.004.

5.11. Application of regression analysis on local scour depth problem

A regression analysis model is used to determine the relationship between a dependent, representing local scour depth, and independent variables, representing the factors affecting local scour depth. According to the equation for vertical wall type:

$$ds/yo = x_{\upsilon o}\ \sigma^{x\upsilon 1}\ \psi^{x\upsilon 2}\ (U_o/U^*)^{x\upsilon 3}$$

$$F_N^{x\upsilon 4}(L/d_{50})^{x\upsilon 5}(L/B)^{x\upsilon 6}K_s^{\ x\upsilon 7}K\theta^{x\upsilon 8}\ . \qquad (13)$$

Where the parameters from $x_{\upsilon o}$ to $x_{\upsilon 8}$ are the regression constants.

The program was run for 71 data sets and the regression parameters were obtained. The equation is:

$$ds/yo = 0.094 \left(\frac{U_o/U^*)^{0.12}F_N^{200}(L/d_{50})^{0.46}(L/B)^{0.10}K_\theta^{\ 1.68}}{\sigma^{0.15}\psi^{0.80}K_S^{0.18}}\right). \qquad (14)$$

Then the equation was applied for the other 71 data sets and the mean was 1.1125 and the standard deviation was 0.26.

5.12. Comparison between ANN model and regression analysis method for vertical wall

As shown in table 10 and fig. 17 that about 96% of the data points are within the range ±25% limit line and for regression analysis results, around 83% of the data points are within the same range. For the range of ±50%, about 97% are within the range ± 50% limit line for the neural model.

For regression analysis results, about 85% are within the range ±50% limit line. By comparing the results, the neural model gives mean 1.04 but regression analysis gives mean 1.12 with increasing ratio 12% the ideal value. The ANN model and the regression analysis give standard deviation of 0.16 and 0.26, respectively. According to these results, it can conclude that ANN estimates more accurate values of local scour depth rather than the regression analysis

5.13. Estimation of local scour depth for wing wall abutment using regression analysis

The program was run for 80 data sets and the regression parameters were obtained. The equation is:

$$ds/y_o = 45.27 \left(\frac{\sigma^{0.34}F_N^{0.718}(L/d_{50})^{0.216}(L/B)^{0.119}}{(Uo/U^*)^{1.35}\ \psi^{0.011}}\right). \qquad (15)$$

Then the equation was applied for the other 78 data sets and the mean was 0.995 and the standard deviation was 0.27.

5.14. Comparison between ANN model and regression analysis method for wing wall type

Table 11 and fig. 18 show that about 72% of the data points are within the range ±25% limit line and for regression analysis results, around 60% of the data points are within the same range. For the range of±50%, about 97% are within the range±50% limit line for the neural model. For regression analysis results, about 96% are within the range±50% limit line. By comparing the results, the neural model gives mean 1.004 but regression analysis gives mean 0.96 with increasing ratio 4% the ideal value. The ANN model and the regression analysis give standard deviation of 0.22 and 0.26, respectively. According to these results, it can conclude that ANN estimates more accurate values of local scour depth rather than the regression analysis.

Table 8
A summary of equations

Kwan [6]	$\frac{d_{sm}}{y_o} = 0.32 + K\left[\frac{L}{y_o}\right]^{0.5}$
Froehlich[9]	$\frac{d_s}{y_o} = 0.78\, K_s\, k_\theta \left(\frac{L}{y_o}\right)^{0.63} F_N^{1.16} \left(\frac{y_o}{d_{50}}\right)^{0.43} \sigma g^{-1.87}$
Melville[2]	$d_s = 2L$ $\quad L/y_o \le 1$ $d_s = 2\,(L\,y_o)^{0.5}$ $\quad 1 < L/y_o < 25$ $d_s = 10\,y_o$ $\quad L/y_o \ge 25$
Lim [7]	$\frac{d_s}{y_o} = K_s(0.9\,X - 2)$
Dey and Barybuiya [3]	$\frac{d_s}{L} = 8.319\, F_e^{0.312} \left(\frac{y_o}{L}\right)^{0.101} \left(\frac{L}{d_{50}}\right)^{-0.231}$

Table 9
Accuracy of Formulas for local scour depth of wing wall type (number of data sets=78

Method	Mean equation (eq.11)	Standard deviation (eq.12)	Percent of data in range		
			0.75-1.25	0.5-1.5	0.25-1.75
Present ANN	1.004	0.22	72	97.43	100
Froehlich eq. [9]	0.79	0.24	46.15	98.72	100
Lim eq. [7]	1.10	0.33	56.41	89.74	97.43
Melville eq. [2]	1.30	0.67	38.46	66.67	80.76
Dey and Barybuiya eq. [3]	1.17	0.38	80.77	85.89	92.30
Kwan eq. [6]	1.37	0.46	39.74	66.67	79.48

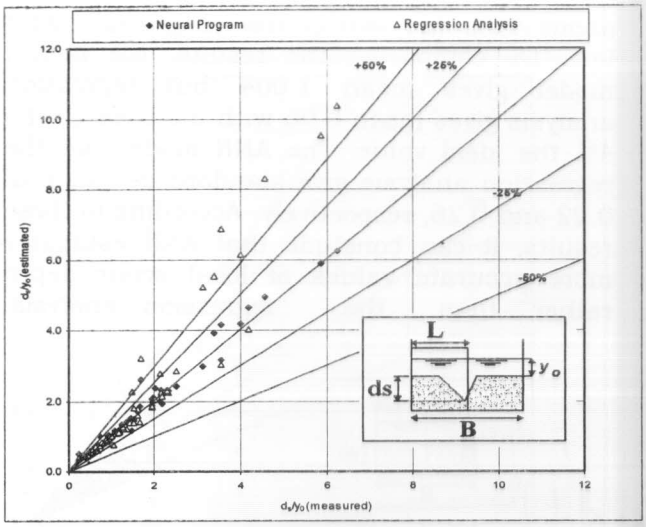

Fig. 17. Comparison between ANN and regression analysis for vertical wall type.

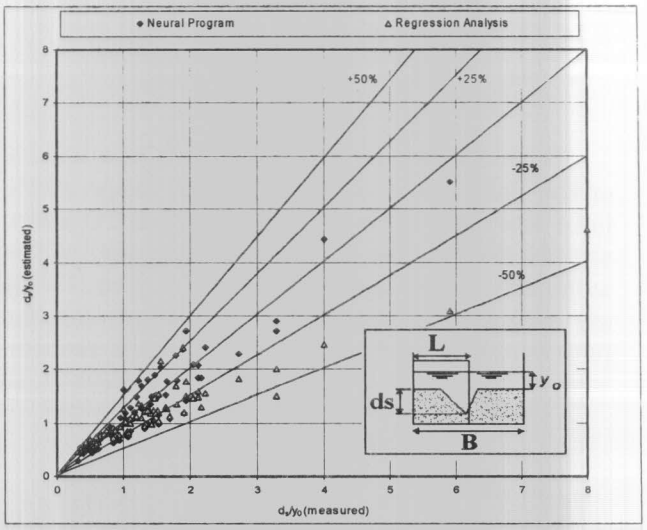

Fig. 18. Comparison between ANN and regression analysis for wing wall type.

Table10
Accuracy of ANN method and regression analysis method for vertical wall type

Method	Number of data	Mean (eq.11)	Standard deviation (eq.12)	Percent of Data in Range		
				0.75-1.25	0.5-1.5	0.25-1.75
Present ANN	71	1.04	0.16	95.77	97.18	98.59
Regression analysis		1.12	0.26	83.10	85.91	95.77

Table 1
Accuracy of ANN method and regression analysis method for wing wall type

Method	Number of data	Mean (eq.11)	Standard deviation (eq.12)	Percent of data in range		
				0.75-1.25	0.5-1.5	0.25-1.75
Present ANN	78	1.004	0.22	72	97.43	100
Regression analysis		0.995	0.27	62	94.87	100

6. Conclusions

Several studies have been conducted to predict the local scour depth around abutments. Most of the methods are based on the regime approach, dimensional analysis, analytical or semi empirical approach. All of these methods depend on much simplification of analysis in order to overcome the complexity of the parameters. In this study, an artificial neural network model was development to estimate the local scour depth.

A feed forward back propagation algorithm was used in the estimation of local scour depth. It also includes a parametric study of the theoretical bases to obtain the dominant parameters of the problem.

Based on the present study, the following conclusions can be obtained:

1. The artificial neural network model gives good agreement with observed values of local scour depth compared with other formulas
2- The artificial neural network model gives better result compared with the regression analysis method.
3- A feed forward back propagation algorithm of artificial neural network model was used successfully in the estimation of local scour depth for both vertical wall type and wing wall type. Before training could be carried out, the size of the networks and the training parameters must be defined.
4- The ANN model has no boundary conditions in application. It does not estimate accurately the scour depth for data out of range of the learning pattern data. Such a problem can easily be overcome by feeding the learning pattern with a wide range of data.
5- By using the artificial neural network model, the effect of different parameters affecting local scour depth can be investigated. For the sensitivity analysis of the model on vertical wall abutment and wing wall types, the basic parameters that affect local scour are Froude number, shear stress and sediment size.

Notation ANN artificial neural network

B is the channel width,
d_s is the scour depth measured from bed level,
d_{50} is the median grain size,
F_N is the froude number,
F_e is the excess abutment Froude number,
K_s is the Melville's shape factor,
Is the Melville's alignment factor,
L is the length of abutment perpendicular to flow,
Q is the discharge of flow,
S_s is the sediment specific gravity,
t is the time to reach equilibrium,
U^* is the bed shear velocity,
U^*_c is the critical shear velocity,
U_e is the approaching velocity,
U_o is the mean velocity of flow,
u_{oc} is the critical velocity of flow,
y_o is the mean flow depth,
α is the shaping ratio of function f,
ν is the fluid kinematical viscosity
ψ is the dimensionless tractive shear stress.
θ is the angle of inclination,
ρ is the fluid density,
σ is the statistical standard deviation, and
σ_g is the sediment geometric standard deviation.

References

[1] M.A. Gill, "Erosion of Sand Beds around Spur Dikes", J. of Hydraulic, Engineering, ASCE, Vol. 98 (9), pp. 1587-1602 (1972).

[2] B.M. Melville, "Local Scour at Bridge Abutments", J. of Hydraulic, Engineering, ASCE, Vol.118 (4), pp. 615-631 (1992).

[3] S. Dey, and A.K. Barbyuiya, "Time Variation of Scour at Abutments", J. of Hydraulic, Engineering, ASCE, Vol.131 (1), pp. 11-23 (2005).

[4] C.B. Tey, "Local Scour at Bridge Abutment", Report submitted to the Road Research Unit of the National Roads Board (329), January, University of Auckland (1984).

[5] K. Kandasamy, "Abutment Scour", Report No (458) submitted to School of Engineering, University of Auckland. (1989).

[6] T.F. Kwan, "A Study of Abutment Scour" Report submitted to the Road Research Unit of the National Roads Board (451), University of Auckland (1988)

[7] S.Y. Lim, Equilibrium Clear-Water Scour around an Abutment", J. of Hydraulic, Engineering, ASCE, Vol.123, (3), pp. 237-243 (1997).

[8] M.M. Rahman and Y. Muramoto, "Prediction of Maximum Scour Depth Around Spur-Dike Like Structures", J. of Hydraulic, Engineering, JSCE, Vol. 43, pp. 623-628 (1999).

[9] D.C. Froehlich "Local Scour at Bridge Abutments", Proceeding of the 1989 National Conference on Hydraulic Engineering, ASCE, New Orleans, LA, pp. 13-18 (1989).

[10] H.M. Nagy, "Maximum Depth of Local Scour Near Emerged Vertical-Wall Spur Dike", Alexandria Engineering Journal, Vol.43 (6), pp.837-847 (2004).

[11] D.E. Rumelhart, G.E. Hinton, and R.J. Williams, "Learning Internal Representations by Error Propagation", Parallel Distributed Processing: explorations in the Microstructure of Cognition, Vol. 1, MIT Press, Cambridge, Mass., pp. 318-362 (1986).

[12] Flood and N. Kartam, "Neural Networks in Civil Engineering.-I. Principals and Understanding:, J. Computing in Civ. Eng. ASCE, Vol. 8 (2), pp. 131-148 (1994a).

[13] M.N. French.W.F. Krajewski and R.R. Cuykendall, (1992) "Rainfall Forecasting in Space and Time using a Neural Network", J. of Hydraulic, Engineering, ASCE, (1992).

[14] H.M. Nagy, K.Watanabe and M. Hirano, "Prediction of Sediment Load Concentration in Rivers Using Artificial Neural Network Model", J. of Hydraulic, Engineering ASCE, Vol. 128 (6), pp 588-595 (2002).

[15] B.M. Melville, "Pier and Abutment Scour: Integrated Approach", J. of Hydraulic, Engineering ASCE, Vol. 123 (2), pp. 125-135 (1997).

[16] M.S. Dongol, "Local Scour at Bridge Abutment", Rep. No. 544, School of Engineering, University of Auckland, Auckland, New Zeland (1994).

[17] M.M. Rahman, M. Murata, N. Nagata and Youshio Muramoto, "Local Scour around Spur-Dike Like Structures and Their Countermeasures using Sacrificial Piles", J. of Hydraulic, Engineering, JSCE, Vol.42, pp. 991-996 (1998).

[18] T.F. Kwan, "Study of Abutment Scour", Report submitted to the Road Research Unit of the National Roads Board (328), January, University of Auckland (1984)

[19] M.Ahmad, "Experiments on Design and Behavior of Spur Dikes", Proceedings International Hydraulics Convention, Minneapolis, Minnesota (1953).

[20] W.H. Wong, "Scour at Bridge Abutments", Report No. 329, School of Engineering, University of Auckland, Auckland, New Zealand (1982).

[21] R. Ettema, "Scour at Bridge Piers", Rep. No. 216, Department of Civil Engineering, University of Auckland, Auckland, New Zeland (1980).

Received March 23, 2006
Accepted November 28, 2006